System level optimisation of Passive Energy Balancing for static and dynamic applications

Alexander D. Shaw * and Michael I. Friswell[†]
Swansea University, Swansea, SA1 8EN, UK

Jiaying Zhang[‡]
Beihang University, China

Chen Wang[§]
Nanjing University of Aeronautics and Astronautics (NUAA), China

Benjamin K. S. Woods[¶]
University of Bristol, Bristol, BS8 1TR, UK

A common issue with morphing structures is that the actuators must work against significant structural and aerodynamic stiffness. The concept of Passive Energy Balancing (PEB) aims to ameliorate this, and thereby reduce system mass, by connecting negative stiffness elements to the actuated degrees of freedom. However, these devices can be complex to design and will also add their own mass to the system. It is therefore difficult to determine the potential for system level mass saving without significant detailed design effort. This work treats a PEB device as essentially a local energy storage mechanism. This frame work leads to an approach to optimisation that will deliver a lightweight PEB mechanism in addition to reducing actuator requirements. It also allows a high level method to obtain an approximate evaluation of system level benefits with only basic information about the application being considered, by comparing general properties of the actuators used to the energy storage properties of the underlying materials used in the PEB device. The work concludes with a case study that shows how the PEB can potentially reduce system mass both through reduced energy consumption requirements and actuator mass savings, and can work particularly well for actuators with non ideal stroke/force profiles.

I. Introduction

The Morphing Aircraft concept seeks to achieve aircraft structures that can change shape in flight, to achieve a better compromises between the competing needs of different flight regimes [1]. Similar concepts are being applied to rotorcraft, to achieve more optimal blade shapes over the highly varied aerodynamic conditions that they experience [2]. In many cases, the morphing occurs at very low frequency, for example at changes in flight condition between approach and cruise for fixed wing aircraft, and changes from hover to cruise for rotorcraft. These transitions occur typically only a few times per mission, and in this work will be referred to as quasistatic morphing. In rotorcraft, there is also a potential requirement to morph more rapidly, at the orders of rotor speed, to counter the varying flow conditions encountered on the blade during forward flight. This can be used to promote efficiency, reduce vibration or even replace complex mechanisms in the rotor hub [3–5]. These more rapid motions can be described as dynamic morphing. The key physical difference between the two is that while the actuation for quasistatic morphing must overcome stiffness (displacement related) and constant forces, dynamic morphing actuators must additionally handle some combination of damping or inertial loads.

Many quasistatic morphing structures work by elastically deforming part of a structure, and therefore actuation must work against the inherent structural stiffness in addition to external loads. This leads to significant weight penalties as

---

*Senior Lecturer, Faculty of Science and Engineering, Bay Campus, Fabian Way, Swansea, UK
[†]Emeritus Professor, Faculty of Science and Engineering, Bay Campus, Fabian Way, Swansea, UK
[‡]Associate Professor, Beihang University, China
[§]College of Aerospace Engineering, Nanjing University of Aeronautics and Astronautics (NUAA), China
[¶]Senior Lecturer, Department of Aerospace Engineering, University of Bristol, UK

actuators are sized to work against the additional structural force. For example, both the fixed wing ADaptive Aspective Ratio (ADAR) wing developed for fixed wing aircraft by Woods and Friswell [6], and the rotorcraft chord morphing concept developed by Majeti *et al.* [2], incur significant structural resistance due to the need to stretch the elastomeric skins to high strains. Passive Energy Balancing (PEB) is a concept designed to alleviate this, by including a Negative Stiffness Mechanism (NSM) in parallel with the structural stiffness, reducing the force and work demand on the actuator. This was introduced by Woods and Friswell [7] where a spiral pulley coupled with a spring induced the necessary negative stiffness, and further developed by Zhang *et al.* [8–11]. In principle, any structure or mechanism that can exhibit negative stiffness behaviour (we could also refer to this as 'bistable' or 'snap through' behaviour) could be exploited in such a device.

However, although it has been shown that PEB can greatly reduce the actuator demand, the system level benefits of this are often far less clear. There is a risk that the negative stiffness mechanism itself will add sufficient weight to eliminate benefits to efficiency at the system level. Indeed, in [11] it was shown that a 50% energy reduction was achieved, at the cost of a 20% increase in mass due to introduction of the PEB, although the resulting potential to then reduce the size of the original actuator was not evaluated.

In early design stages, it is highly undesirable to require a complete detailed design of components before the likely performance and system level benefits are clear. Therefore, high-level models of PEB are needed that can give reasonable predictions without the need for detailed design. Then if an approximate high level analysis predicts significant system level advantages for a reasoanbly well optimised system, the detailed design process can proceed. A similar goal has been achieved for conventional actuators, whereby decisions can be based on initial actuator data without detailed design and justified using plots of actuator properties and indices [12–14].

This work develops such an idea, by considering a PEB system as an energy storage device, sized principally by the amount of elastic potential strain energy that it stores. In Section II the simplest case of actuation against a pure stiffness-type loading is studied. An approach to optimising the PEB device, that treats the stored elastic potential strain energy as a proxy for overall mass, is developed. The required performance of the PEB device is specified in terms of the required actuator force or work reduction. Then the PEB device is optimised to achieve the required performance with the minimal requirement for elastic energy storage. It is also shown that the material used for the energy storage part is a crucial consideration, and that this leads to an index based approach for material choice and approximate evaluation of the likely benefits of PEB.

Section III shows how this analysis can be used to give first order estimates of system mass saving. Section IV presents a case study of PEB applied to the Transition Induced Camber (TRIC) morphing concept [15, 16], where it is shown that it works particularly effectively for actuators with low stroke work coefficients. Finally, conclusions are discussed in Section V.

II. Quasistatic actuation against pure stiffness loads

A. An SDOF analysis of the force and work saving due to a PEB with nth power nonlinearity

Assume a simple, single degree of freedom actuation scenario as illustrated in Fig. 1, where an actuator drives a single elastic load between 0 and a maximum displacement x_0. In this scenario, the actuator must be able to provide a force given by:

$$f(x) = P_s(x) + P_n(x) \ . \tag{1}$$

Ideally the negative stiffness device could be chosen so that $f(x) = 0$ for all x. This can sometimes be achieved with a Spiral Pulley negative stiffness mechanism, which allows great flexibility in shaping nonlinearity through the choice of spiral pulley profile [7, 9]. However many mechanisms only have a couple of parameters that can be altered so this is not always feasible in practice. Furthermore, no structure exhibits negative stiffness over an unbounded range. Instead, negative stiffness is found in a limited range, bounded by regions of positive stiffness and two equilibrium points in structures exhibiting bistability. The force displacement curves of bistable structures come in many different forms, but for the sake of simplicity let us initially assume the form:

$$P_n(x) = k_1 x + k_p x^p \ , \tag{2}$$

noting that this will have negative stiffness around $x = 0$ if $k_1 < 0$. In this mathematical example, the 'designer' has control of constants k_1, k_p and p. Let us further assume the PEB is placed in parallel with a linear elastic structural load given by:

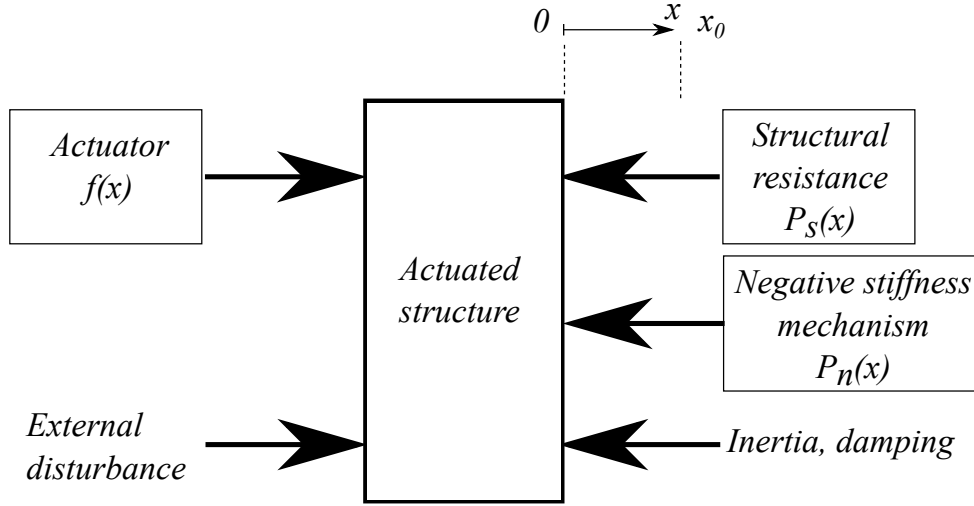$$P_s(x) = k_s x \ , \tag{3}$$

Fig. 1   Diagram of the generalised case of actuation - the actuator drives an elastic load. A negative stiffness mechanism is placed in parallel with the structural stiffness, driving the combined stiffness toward zero and reducing the duty of the actuator. Further forces that are neglected in the quasistatic analysis are also shown for completeness.

as shown in Fig. 2.

The result is plotted in Fig. 3 for $k_s = 1$, $k_1 = -1$, $p = 3$, $k_p = 1$. It is clear that the usefulness of the NSM depends on our required stroke x_0; at low values (< 0.5) the actuation requirement is reduced to almost zero. The NSM provides a maximum reduction in force at $x = \pm\frac{1}{\sqrt{2}}$. However, it can be seen that the NSM force displacement function has additional zeros at $x \pm 1$, and outside of this range the NSM increases the required force that the actuator must supply. Note, that in this region the stiffness is actually increased, in contrast to the reduction in stiffness near zero, and this could have some benefits to the stability of the system when fully actuated.

Considering the graph of work in Fig. 3 (b), which is readily found by integrating the force functions against displacement, the limits of usefulness are broader - the NSM actuator is required to provide less work than the unassisted actuator until just above $x = \sqrt{2}$. However the *maximum* benefit in terms of work is in this case achieved at $x = 1$. This maximum work is denoted U_{max} and this is to be taken as the maximum useful work a given NSM can contribute towards actuation. One indicator of the optimality of the NSM is the ratio β of work actually provided at the target stroke x_0, to the total energy that the NSM can store, given by

$$\beta = \frac{U_0}{U_{max}} , \tag{4}$$

where U_0 is the stored strain energy at the chosen stroke x_0. Ideally, β would be unity, indicating that all stored energy is used, but in most cases it will be greater.

B. Optimising based on stored work

If the fundamental role of the PEB device is a means of storing and releasing a certain amount of potential energy on each actuation cycle, and that it is sized by the amount of energy stored, two design principles immediately follow. Firstly, that no more energy than is necessary should be stored, because to do so would introduce excess mass. Secondly, the storage medium, in terms of the elastic structure used, should be designed with a material and structure that maximises the energy stored per kilogram of mass. The material and structure for the energy storage medium is discussed in Sections II.C and II.D respectively.

This section addresses the first point above, by describing a series of different strategies for choosing a nonlinear function for the NSM that optimises stored energy. These strategies are described in subsections II.B.1 to II.B.3, and then compared in summary form in subsection II.B.5. Note that all strategies give significant stiffness nonlinearity in the range of interest; no true device gives fully linear negative stiffness over an infinite range, as this would require infinite
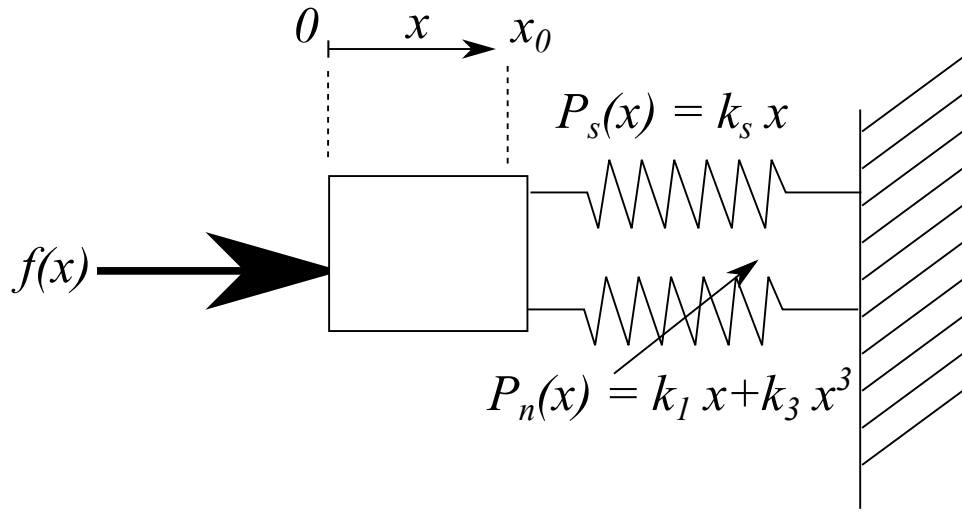
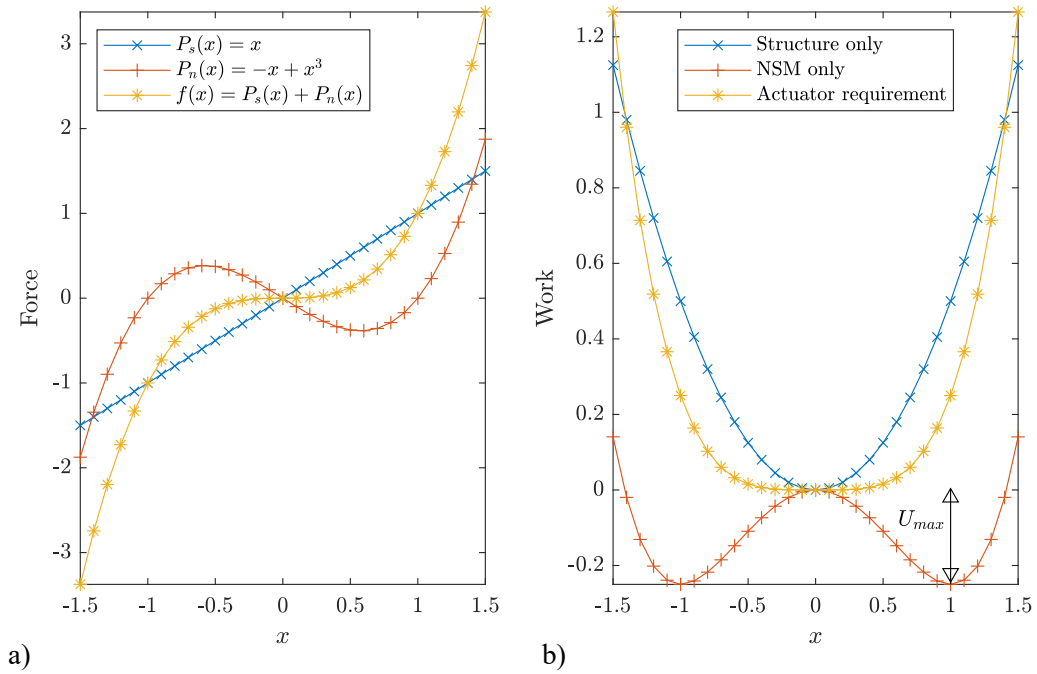**Fig. 2   A linear elastic structure with a cubic NSM.**

a)   b)

Fig. 3   The effect of a cubic NSM on a linear elastic load in terms of both force and work.

energy to be stored. It follows from this that even to give near-linear behaviour over the actuation range would require a potentially excessive amount of energy to be stored, and therefore a likely outsized device. Therefore, nonlinearity is an essential feature of an optimal PEB device.

In summary, this section uses the stored elastic energy as a proxy for the mass of a PEB device. This assumption is reasonable so long as the material for the underlying elastic medium is assumed to always be worked to near its maximum elastic energy density.

1. Setting the stored energy equal to required work

It seems reasonable to match the stored energy exactly to total needed for actuation, by solving

$$\int_0^{x_0} P_n(x)\mathrm{d}x + \int_0^{x_0} P_s(x)\mathrm{d}x = 0 \ . \tag{5}$$

Referring to Fig. 3 and related discussion that shows that the maximum work benefit comes at the turning point of the energy graph, therefore to have an isolator that stores no more energy than strictly necessary we can set a condition that

$$P_n(\pm x_0) = 0 \tag{6}$$

which when using Eq. (2) gives:

$$k_1 = -k_p x_0^{p-1} \tag{7}$$

Secondly, substituting Eqs. (2) and (6) into Eq. (5) leads to

$$k_p = \frac{k_s(p+1)}{x_0^{p-1}(p-1)} \tag{8}$$

When we consider Fig. 4, we see there are potential problems with this approach. The approach gives an overall stiffness around $x = 0$ that is negative, which could be undesirable, unless the stiffness of the actuator itself is sufficient to maintain overall stability. Furthermore, this approach doesn't quite deliver 'zero work' because the actuator cannot store the work returned, so the actuator must still provide a little work near the maximum range, around 0.12 for $p = 3$. This reduces as p increases, but increasing p also widens the region of negative stiffness. Another feature is that there is no reduction in the actuator force at x_0. A positive benefit from this design is that stiffness is actually increased near $\pm x_0$.

In summary, this design could work well, however it does not quite deliver its stated aim of zero work and the negative stiffness of the overall structure may be a problem.

2. Zero stiffness and no unused stored energy.

If negative stiffness in the overall structure is unacceptable, then it seems sensible to set a further constraint that stiffness is zero at $x = 0$, by choosing $k_1 = -k_s$. To ensure that all energy in the NSM gets used, Eq. (7) is used to choose k_p, giving the results in Fig. 5. This approach leads to an actuator that must do more work, but a smaller negative stiffness device, because less energy is stored. As p increases, the energy stored increases; for $p = 3$ the actuator must still do 50% of the overall work. Again there is increased stiffness at $\pm x_0$, but no reduction in the actuator force required at x_0. In summary, this approach works but delivers relatively little stored energy with the forms of nonlinearity considered here.

3. Zero stiffness, 90% work contribution

A further way of designing this could be to aim for a high percentage of the actuator work to be supplied by the negative stiffness, and to avoid bistability set overall minimum stiffness to zero. This approach could be considered to be pragmatic, because even if all force and work is eliminated, an actuator is still needed on a real system, so it might as well do a small proportion of the work. Note also, that if you attempt to supply 100% of the available work with zero stiffness you need a linear negative stiffness, which is impossible.

The requirement to meet condition (7) is relaxed, and the condition

$$\int_0^{x_0} P_n(x)\mathrm{d}x + \alpha \int_0^{x_0} P_s(x)\mathrm{d}x = 0 \tag{9}$$

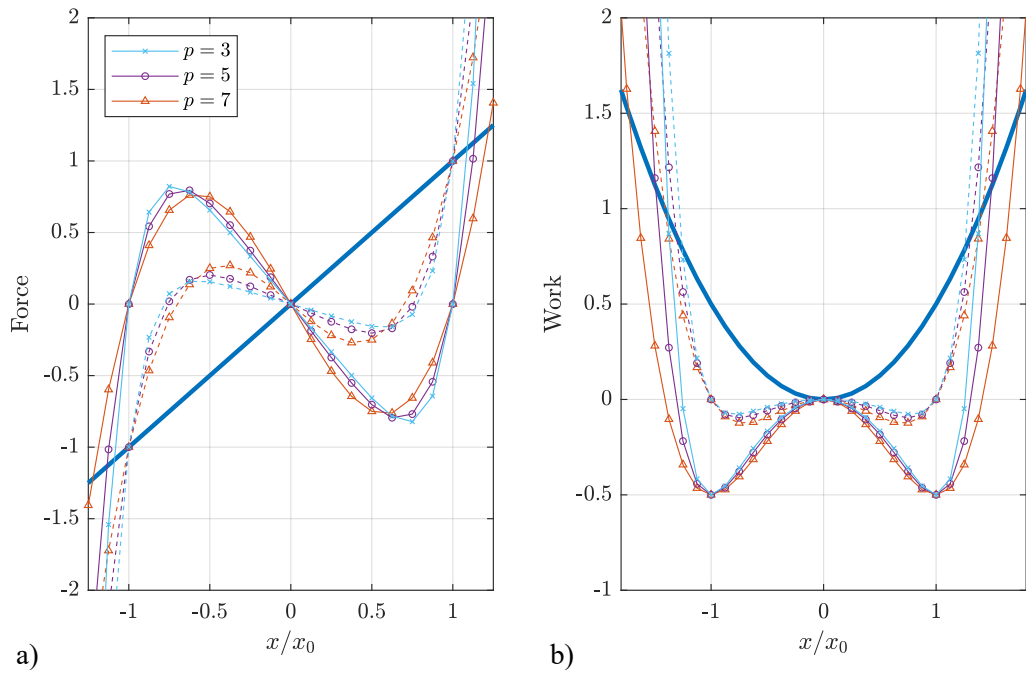**Fig. 4** **Force and work for $p = 3, 5, 7$, 'zero work' design. Bold line: underlying structure. Solid line: negative stiffness device. Dashed line: total work/force for actuator.**

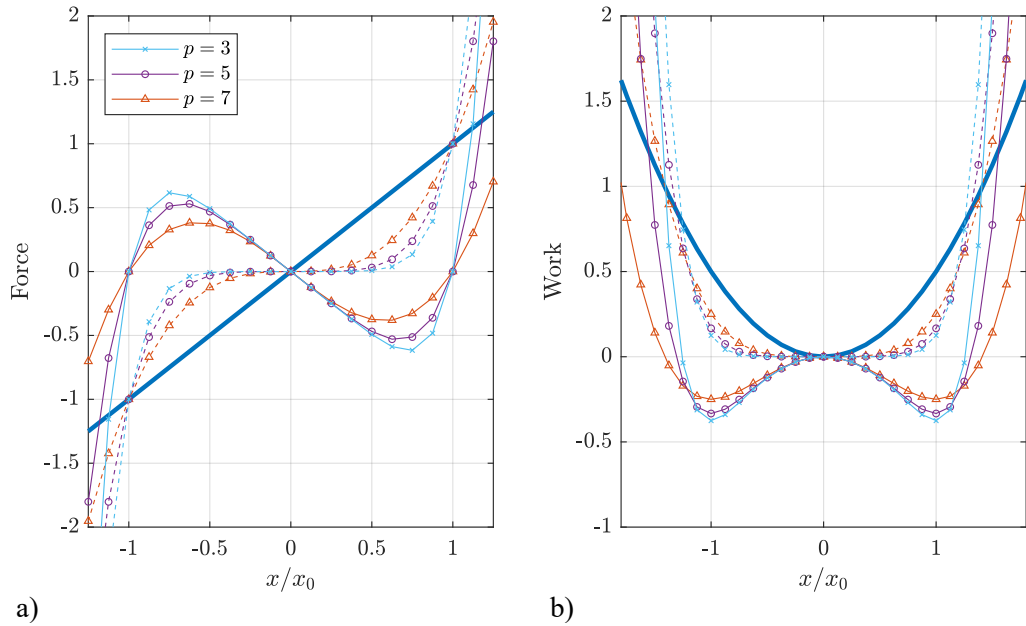**Fig. 5** **Force and work for $p = 3, 5, 7$, 'zero stiffness' design. Bold line: underlying structure. Solid line: negative stiffness device. Dashed line: total work/force for actuator.**
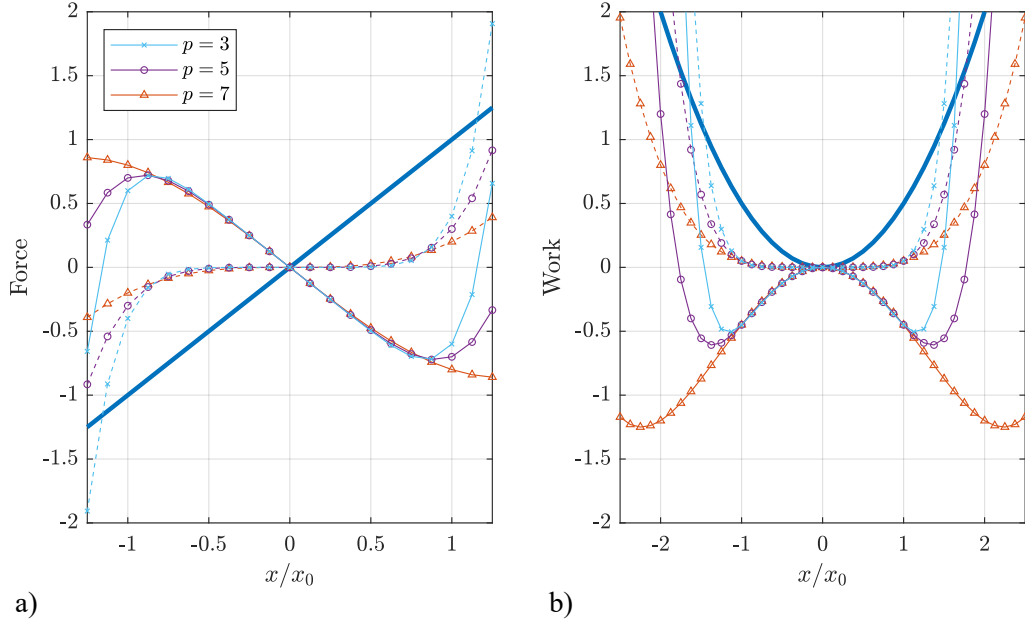
Fig. 6 **Force and work for** $p = 3, 5, 7$**, '90% work' design. Bold line: underlying structure. Solid line: negative stiffness device. Dashed line: total work/force for actuator.**

where $\alpha = 0.9$ is enforced by substituting Eq. (2) into Eq. (9) to get

$$k_p = k_s (\alpha - 1) \frac{p + 1}{2x_0^{p-1}} . \tag{10}$$

This approach guarantees a lot of actuator work reduction, but also a larger heavier negative stiffness device, because it stores some potential energy that it doesn't use. The results in Fig. 6 show that in the case of $p = 3$, the NS device stores over twice the strain energy that is actually supplied to the actuator, although this improves rapidly as p increases. The approach can be readily adapted to choose different proportions of stored work by varying α. It can also be seen that this method reduces the peak force required at x_0.

4. Specifying the reduction in peak force.

In many cases an actuator is sized by maximum force requirement rather than work output. In this case, the focus should clearly be on reducing the peak force, whilst still minimising the requirement to store energy. To do this, the minimal force point of the negative stiffness function should be located at x_0 by ensuring that

$$\left. \frac{dP_n}{dx} \right|_{x_0} = 0 \tag{11}$$

which for an NSM with form of Eq. (2) gives

$$k_1 = -pk_p x_0^{p-1} . \tag{12}$$

A chosen reduction in force is obtained by solving

$$P_n(x_0) = -f_0 , \tag{13}$$

where f_0 is the desired amount of force reduction. In the case where $P_n(x)$ is of form Eq. (2), this leads to $k_p = \frac{f_0}{x_0^P (p-1)}$.

The results of this approach are shown in Fig. 7. As expected, this result requires more stored work than the others, and again the higher nonlinearity reduces the stored work.
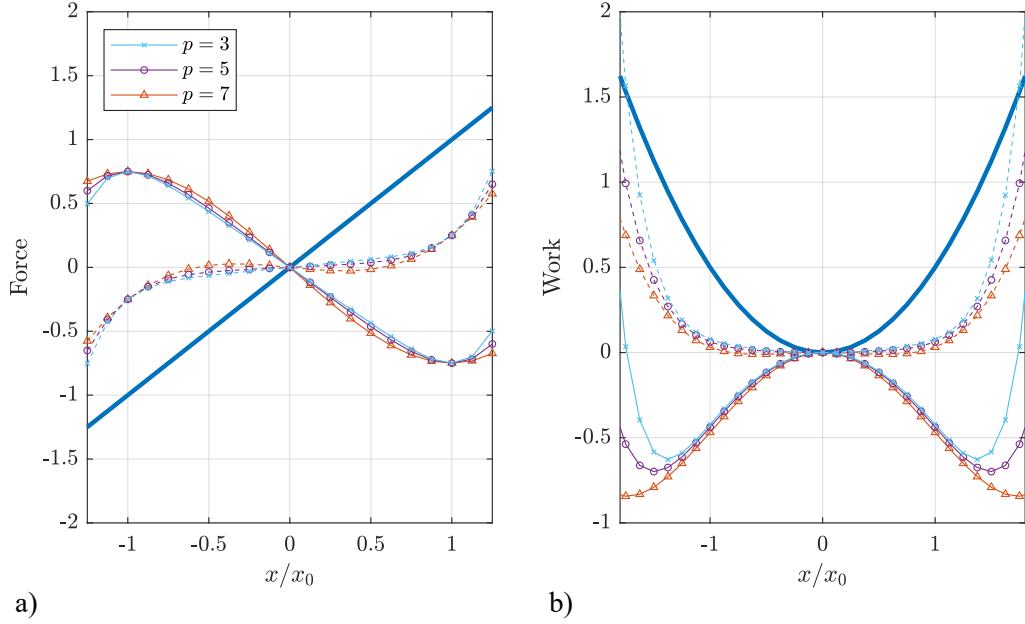
7

Fig. 7 **Force and work for** $p = 3, 5, 7$**, with peak force set to 25% of the unassisted value. Bold line: underlying structure. Solid line: negative stiffness device. Dashed line: total work/force for actuator.**

5. Summary comparison of approaches to optimising nonlinearity and energy storage

Table 1 shows a comparison of the different approaches to designing the NSM. Note that the actuator work column, assumes that the actuator cannot recover work from the system, and so does not benefit from regions of negative stiffness. Increasing p reduces stored work in all cases, however note that the problem of high excess energy storage in the 90% method is greatly reduced by choosing a slightly lower proportion of stored energy when $\alpha = 0.8$ is chosen. Note that in this nondimensional study, the unassisted system would need actuator work to be 0.5, so in the majority of cases the storage mechanism stores more energy than the actual stroke work.

For the maximum force reduction case, the stored work is generally higher than all other cases, except for the '90% work' method for $p = 3$. Note that in this case, the actuator has to supply very little work, although this work increases with nonlinearity p. However increasing p reduces the stored work and therefore the PEB size significantly. A further conclusion is that the force reduction case also reduces actuator work very considerably, so in general the aim of force reduction is not strongly in opposition to the aim of work reduction.

C. Material for energy storage.

Regardless of the form of the elastic storage mechanism (ie. spring, beam etc), the ability to store energy is determined by the material that it is made from. It therefore follows the energy storage material should be the initial consideration in the design of an NSM, and the material properties alone can give insight into the potential performance limits of the mechanism.

The energy density of a Hookean material under uniaxial load is given by

$$e = \frac{1}{2}\sigma\epsilon \ . \tag{14}$$

This gives the specific energy of the stressed material if divided by mass density

$$u = e/\rho = \frac{\sigma\epsilon}{2\rho} \ . \tag{15}$$

The maximum value of specific energy will occur when the material is working as hard as it can, ie. near its maximum

8

Table 1   Table comparing different approaches to optimising the NSM based on energy storage.

Optimisation method	Actuator work ($p = 3, 5, 7$)	Stored work ($p = 3, 5, 7$)	Negative stiffness	Effect on stiffness at full stroke	Effect on force at full stroke
'zero' work	0.1250, 0.0962, 0.0787	0.5 0.5 0.5	yes	increases	none
'zero' stiffness	0.2500 0.1667 0.1250	0.2500 0.3333 0.3750	no	increases	none
90% work reduction	0.05 0.05 0.05	1.2500 0.6086 0.5090	no	increases except for $p = 3$ which decreases	reduces
80% work reduction	0.1 0.1 0.1	0.6250 0.4303 0.4040	no	increases	reduces
75% force reduction	0.0312 0.0625 0.0781	0.8438 0.6988 0.6277	possibly	unchanged	reduces

allowable stress. Furthermore we can rearrange Hooke's law to obtain

$$u_0 = e_0/\rho = \frac{\sigma_0^2}{2E\rho} \ , \tag{16}$$

where σ_0 is some measure of allowable stress. In practice σ_0 would be limited by fatigue characteristics but if we assume for simplicity that it is related to the yield stress σ_y of the material, we can use the material index $\frac{\sigma_y^2}{2E}$ as an indicator of maximum energy density and plot this for various materials against ρ to get a strong indication of which materials are most suitable for this role.

The value $\frac{\sigma_y^2}{2E}$ has been plotted against density in Fig. 8 for general classes of materials, using Granta Edupack software [17]. It is clear that elastomers hold a significant lead over other materials, although properties of these materials such as hysteresis, creep, nonlinearity and temperature sensitivity may complicate their use in practice. Steel materials are seen to have specific strain energy on the order of 1 kJ/kg.

D. Structural form of the energy storage mechanism

Engineering structures do not necessarily feature constant stress, as usually they have a variable distribution of stress. That means the benefits of the full specific energy density that the material can achieve is seldom seen. Archetypal examples of engineered structures for storing energy, that can potentially be exploited in NSMs, include axially loaded (unbuckled) rods, loaded springs and beams under bending loads as shown in Fig. 9. Of the examples shown, only pure tension or compression achieves a uniform stress distribution throughout out all material, suggesting that this may in theory be the most efficient configuration. However, this configuration could be prone to buckling (if in compression) and in either case would require high restraint forces at each end, which could result in large and heavy supporting structure. The other cases show a linear distribution of stress with either through thickness position or radius as appropriate; in the case of bending the neutral axis has no stress at all and in the case of torsion (the primary means by which a coil springs stores energy) the centre of twist has no shear stress. It can be shown that the *average* specific energy of a beam in bending per unit length is given by

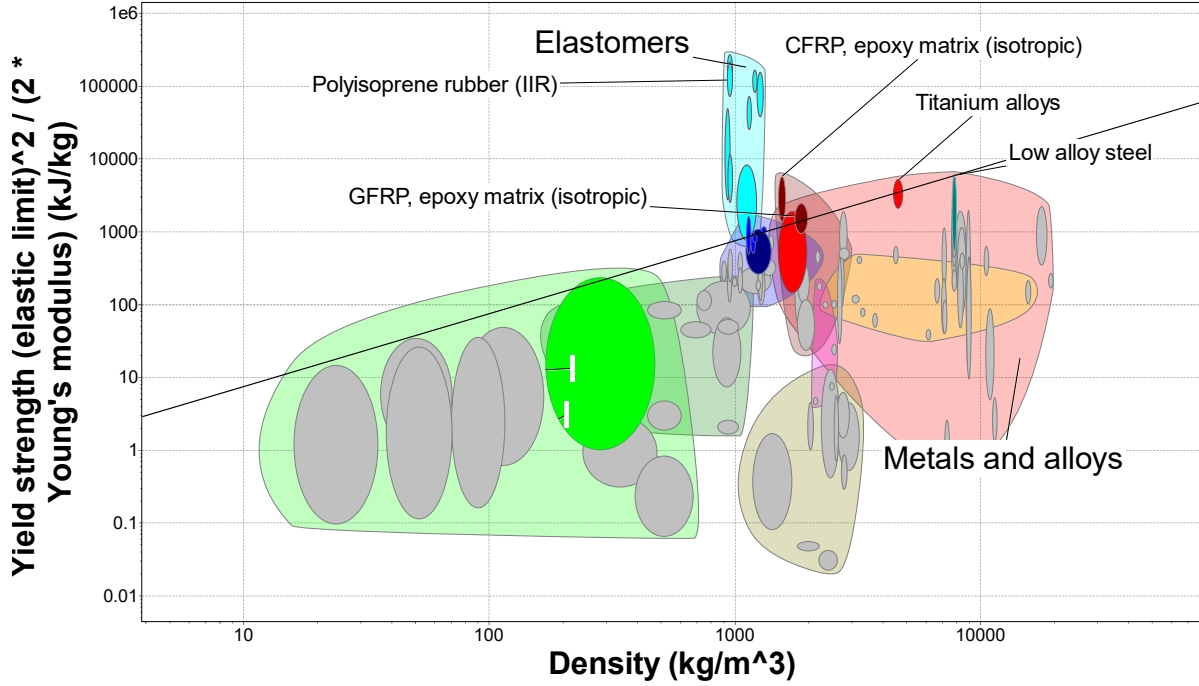$$\bar{u}_{bending} = \frac{\sigma_0^2}{6E\rho} \tag{17}$$

9

Fig. 8 Plot of $\frac{\sigma_y^2}{E}$ against density for numerous materials. Line indicates materials with equal specific strain energy to Low Alloy Steel. Image used courtesy of ANSYS, Inc.

and that for a rod in torsion it is given by

$$\bar{u}_{torsion} = \frac{\tau_0^2}{4G\rho} \,, \tag{18}$$

where σ_0 and τ_0 are the maximum direct and shear stresses respectively. Equations (17) and (18) show that the bending and torsion deformations store on average 2 or 3 times less energy than the bulk material will allow when in a state of direct axial stress.

III. Mass saving at a system level

A conventional actuator adds mass to a system through three means[13]:
1) The mass of the energy source from which the actuator is ultimately powered
2) The actuator mass itself
3) The mass of means to connect power to the actuator and any power conversion devices needed

Items 1 or 2 can both be potentially sized by the required actuator work. Item 3 is arguably almost always sized by power, and is not considered here. The following sections discuss the potential system level impact of PEB when actuators are sized by quasistatic work requirements.

A. Energy source mass saving

The mass of an energy source required to perform N cycles of actuation is given by:

$$m_f = \frac{NU}{u_f \eta} \tag{19}$$

where u_f is the specific energy of the energy source, U is the overall work of the required motion and η is the efficiency of conversion from fuel source to final work output. The mass of the NSM is assumed to scale with required energy hence $m_n = \frac{\alpha U}{\bar{u}_n}$, where $0 < \alpha < 1$ is the proportion of work provided by the NSM, and $\bar{u}_n$ is the specific strain energy of
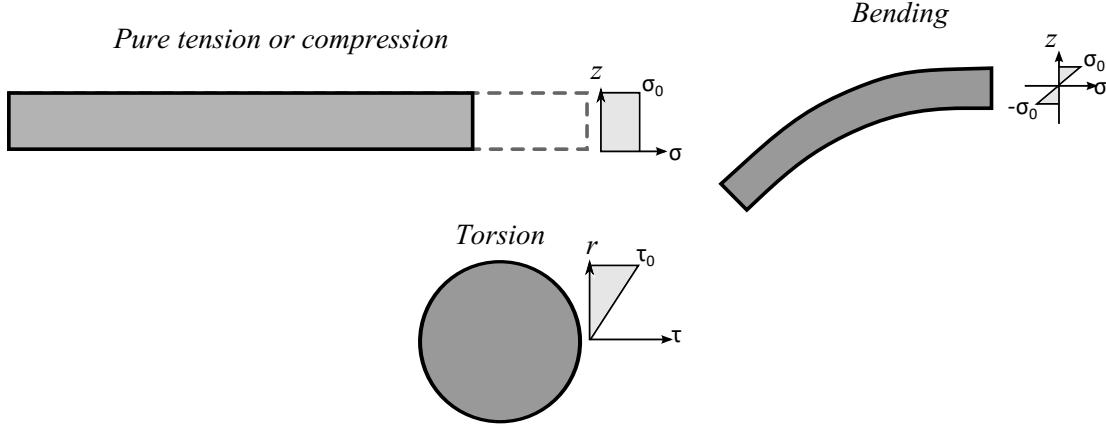
Fig. 9   Stress distributions for some typical deformations.

the NSM, which is of the order (u_0/β), where u_0 is the maximum specific strain energy for the energy storage material, and β is given by Eq. (4). Hence the overall change in mass is:

$$\Delta m = \alpha U \left(\frac{1}{\bar{u}_n} - \frac{N}{u_f \eta} \right) \tag{20}$$

For the change in mass to be negative as desired, the bracket must be negative. The specific energy of most energy sources is far greater than mechanical energy storage, so there will be a threshold of N where the presence of the ideal PEB leads to a weight saving over the course of a mission.

Kerosene has a specific energy on the order of 43 MJ/kg [18], which is 4 orders of magnitude greater than typical steel based energy storage, even when losses in conversion to mechanical energy are considered . Therefore, a NSM using steel springs for energy storage in a kerosene powered aircraft is likely to need over 10,000 cycles per mission before it provides a net saving in terms of fuel reduction. If we consider a typical rotorcraft mission, a B105 Helicopter (currently produced by Airbus Helicopters), operating for an hour with a rotor speed of 7Hz, then this approximately gives 25,200 rotations per mission. Therefore there is a reasonable chance that assisting an active flap actuation that operates 1 to 2 times per rev will result in system level fuel saving, but of course this benefit could be eroded by the additional PEB mass and complexity. If the energy storage exploited elastomers, which have two orders of magnitude better specific energy than metals, this analysis suggests that fuel saving may be even greater. However, this neglects any potential losses associated with elastomer phenomena such as hysteresis and creep, and so this conclusion should be treated with caution.

B. Actuator mass saving

Figure 10 shows an equivalent metric to Eq. (16) but applied to actuators, following [12], and is generated using Granta Edupack software [17] with an additional actuator database available at [19]. The work per unit volume of the actuator is presented in terms of derived actuator properties, actuator stress, actuator strain and the stroke work coefficient explained in [12], and this is plotted against actuator density in an equivalent manner to Fig. 8.

It is clear that specific actuator work can take a wide range of values, both above and below the specific elastic energy of steel which has an order of magnitude of 1 kJ/kg. Some actuators feature exceptionally high work densities, and these include pneumatic and hydraulic actuators. In these cases,a steel based PEB is unlikely to lead to system level mass saving due to reduced actuator size, because the actuator delivers work more efficiently than the PEB can store energy. However there are many cases where these actuation systems are not feasible, in particular when we consider installation in helicopter blades. However, many actuators have specific work capacities that are orders of magnitude lower, and in these cases it can be concluded that a steel PEB has a strong likelihood of reducing the overall mass of the actuation system.

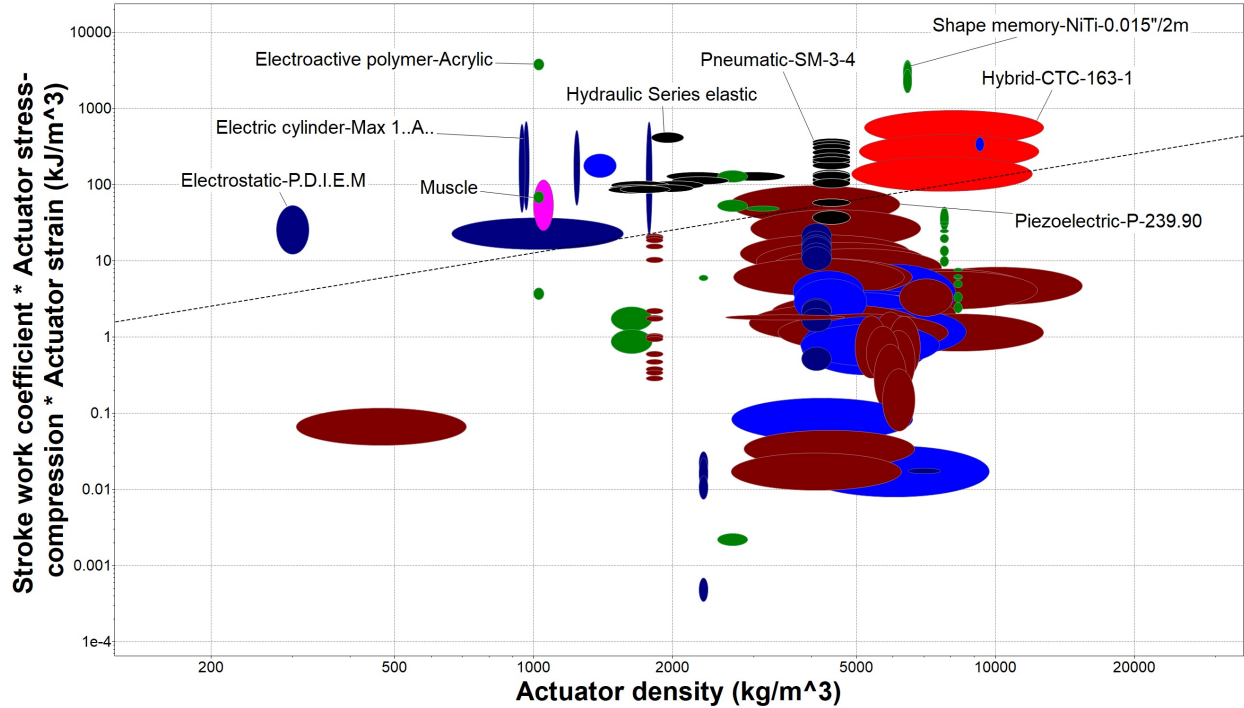## IV. Case study: Actuation for TRIC morphing

Fig. 10   Actuator work density versus actuator mass density for a range of actuators. Dashed line shows a line of constant specific actuator work capacity. Image used courtesy of ANSYS, Inc.
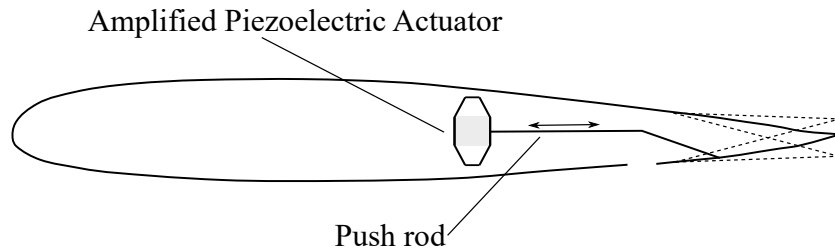

Fig. 11   TRIC concept

A. Background

The Transition Induced Camber (TRIC) concept is a method for camber morphing of an aerofoil [16, 20], shown schematically in Fig. 11. It has been proposed for active blade applications in rotorcraft [15].

It has been proposed that a CEDRAT APA 1500 L amplified piezoelectric actuator [21] is used to drive the mechanism, due their high bandwidth, blocking force, stiffness and general suitability for use in the rotor environment [15]. Some data for the actuator is given in Table 2. The load to be driven consists of a combination of structural and aerodynamics forces but is essentially linear and elastic.

A typical stroke force relation for the actuator has the form shown in Fig. 12; there is no available force at maximum stroke and no stroke available at maximum force. In other words, it has a stroke work coefficient of 0.5 [12], compared to 1 which is seen in ideal actuators such as hydraulic pistons. This means it can only practically output 50% of the work suggested by the product of its maximum force and maximum stroke; against a linear elastic load the maximum work output is even less as shown in Fig. 12. This issue is common to many piezoelectric actuators [12]. Assuming a constant resisting load, the maximum work output is found at a stroke and force that is half of the maximum stroke and maximum force respectively. Because the target load is linear elastic, maximum force is required at maximum stroke for the morphing application concerned. This has led to the developers of the TRIC concept employing 2 actuators in

Table 2   Data for the CEDRAT APA 1500 L actuator.

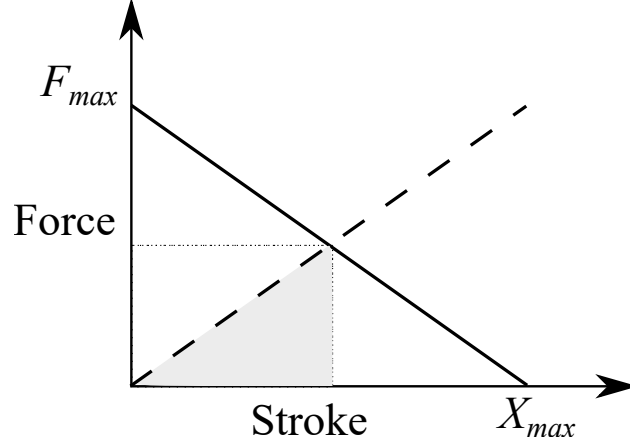| Maximum stroke	1480 μm
Blocked force	99 N
Stiffness	0.07 N / μm
Mass	143g

Fig. 12   Solid line: Typical force displacement profile of piezoelectric based actuators. Dashed line: a linear elastic load requirement. Shaded area represents the output work for a linear elastic load.

series in the current design iteration, so that the required force is achieved with a reasonable stroke. This case study will consider whether PEB offers a potentially improved actuation solution.

B. Initial feasibility of PEB

As an initial consideration, we should simply compare the work density of the actuator to the potential specific elastic energy storage capacity of a typical PEB. We can directly calculate the nominal work per mass of this actuator, which from the data in Table 2 gives 0.1465 J/kg. In fact, if the stroke work efficiency of the actuator is considered, this value becomes 0.0773 J/kg. This is 4 orders of magnitude smaller than the value quoted for the specific elastic energy of steel. In combination with our assumption that the target load behaves in an elastic fashion, this confirms that there is a strong initial case for PEB achieving a system level mass saving in energy terms. In the next subsections we do some initial design on a PEB mechanism, and see if potential benefits on this scale are likely to be realised.

C. PEB design concept

A simple PEB mechanism based on snap through springs, as shown in Fig. 13 is proposed. This mechanism is chosen for its simplicity as it needs to operate with high reliability in the highly vibratory and high-g environment of the helicopter blade. It consists of two precompressed springs coupled to the linear motion of the actuator. The springs have initial length ℓ_0, but when the actuator is at zero displacement they are compressed to a length of a. If each spring has stiffness k, the elastic strain energy of the PEB system is given by

$$U = k \left(\ell_0 - \sqrt{a^2 + x^2} \right)^2 . \tag{21}$$

Differentiating Eq. (21) leads to the force displacement function for the PEB:

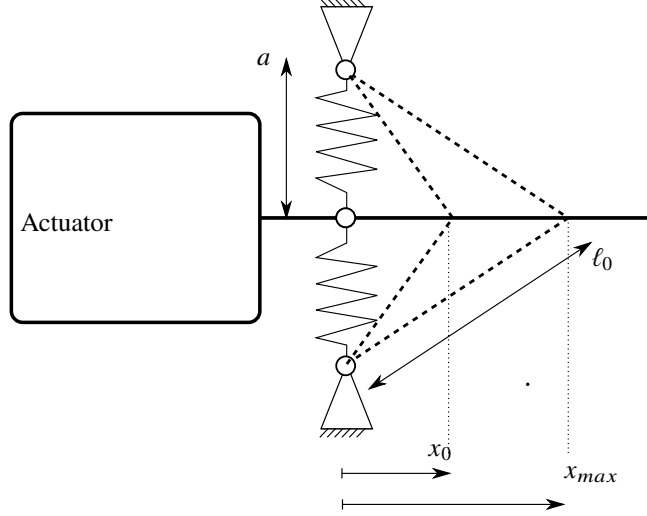$$P_n(x) = 2kx \left(1 - \frac{\ell_0}{\sqrt{a^2 + x^2}} \right) \tag{22}$$

13

Fig. 13   Schematic of proposed PEB mechanism.

D. PEB optimisation

In order to allow the actuator to achieve a higher stroke, we are treating this as a force limited problem; by reducing the actuator force to a fraction of the unassisted value it will increase the available range. The following design process ensures a near optimal snap-through PEB.

In order to ensure that the two springs are exploiting the materials' energy storage to somewhere near its limit, we assumed that at $x = 0$ they are compressed to half of their original length, ie. $\hat{a} = a/\ell_0 = 0.5$. This ensures the spring is being exploited to near maximum energy, whilst also keeping to reasonable value for the maximum stretch of a spring. Note that a higher $\hat{a}$ could be chosen, giving a heavier spring, although using less extreme deformation could be beneficial if the fatigue life of the spring is a limiting factor.

The next step is to ensure that the greatest magnitude of force is located at the desired stroke x_0, by solving Eq. (11) using the form of $P_n(x)$ given in Eq. (22). It is shown in Appendix A that the nondimensional value $\hat{x}_0 = \frac{x_0}{\ell_0}$ that gives greatest force assistance is found as the real root of

$$\hat{x}_0^6 + 3\hat{a}^2\hat{x}_0^4 + 3\hat{a}^4\hat{x}_0^2 + \hat{a}^6 - \hat{a}^4 = 0 \ . \tag{23}$$

Once this is known, it can be used to choose $\ell_0 = \frac{x_0}{\hat{x}_0}$.

Finally, it simply remains to choose the spring stiffness k, by matching the required force reduction f_0 at x_0 using

$$k = \frac{f_0}{2x_0 \left(1 - \frac{\ell_0}{\sqrt{a^2 + x_0^2}}\right)} \ . \tag{24}$$

The above process ensures a PEB with (i) spring elements highly compressed but within safe limits as chosen by the designer and (ii) maximum force reduction at the required stroke for the given amount of elastic strain energy.

E. Results of optimisation

The above process is applied to a linear elastic load where the peak force and displacement are 50 N and 1.5 mm respectively. This is the force and stroke supplied by 2 APA 1500L actuators placed in series as described in [15], with the actuators working near their optimal work output. The snap through mechanism is designed to reduce the peak force at the actuator by $f_0 = 40$N.

The resulting properties are given in Table 3. As can be seen the resulting mechanism has a size on the order of the required displacement, which in this case is very small.

14

	$\hat{a} = 0.5$	$\hat{a} = 0.8$
k kN /m	22.7	83.1
ℓ_0 mm	3.91	4.68
a mm	1.96	3.74

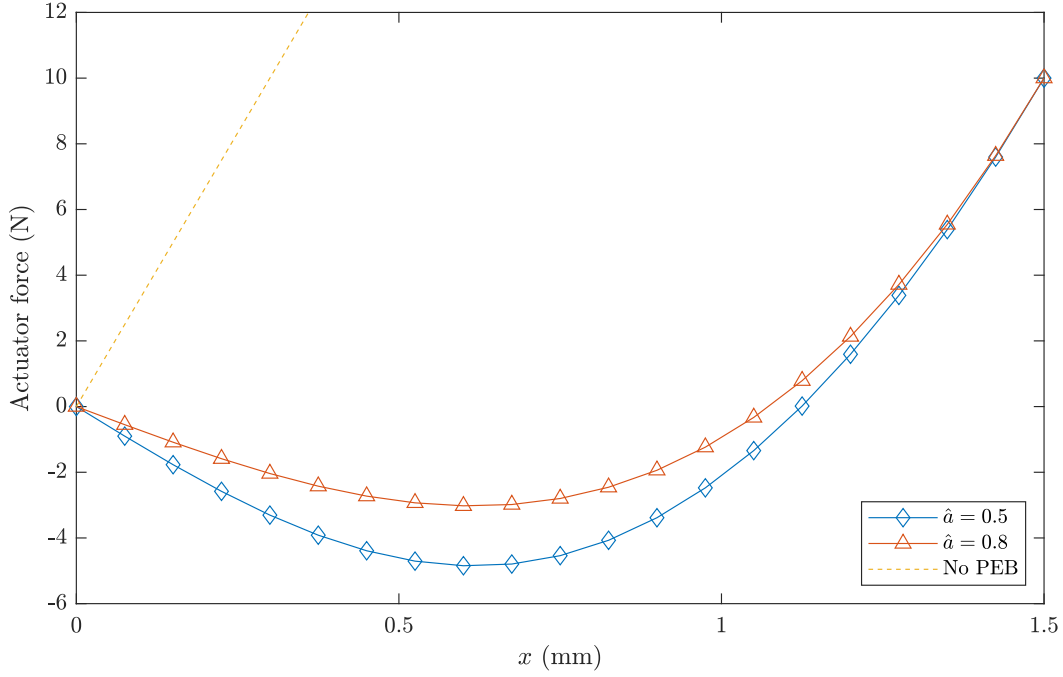**Table 3   Results of PEB optimisation.**

Fig. 14   The actuator force when assisted by the PEB device.

It finally remains to be verified that the required spring properties can be achieved. Table 4 show some spring dimensions where the formula

$$k = \frac{Gd^4}{8ND^3} \tag{25}$$

has been used to design coil springs with the rate and length required, where G is the shear modulus of steel, taken to be 76.9 GPa, d is the diameter of the wire used for the spring, N is the number of loops and D is the winding diameter. This table shows that the required properties are near the limit of what can be achieved with a coil spring architecture, but more sophisticated geometries could produce better solutions.

The modified force displacement curves that the actuator experiences are shown in Fig. 14. It can be seen that the $\hat{a} = 0.8$ case has slightly less nonlinearity than for $\hat{a} = 0.5$, and this case uses the lighter springs of the two, reinforcing the general trend that nonlinearity is beneficial to mass. Note also that both curves feature some negative stiffness, but referring to Table 2 we see that the self stiffness of the actuator is more than sufficient to overcome this and prevent instability.

F. Implications of PEB implementation

The assistance of the PEB can be exploited in a number of ways for this system. The first way would be to allow a greater spacing of actuators along the span of the rotor blade, because now the actuators are assisted by PEB they can deliver more force. A second way is to note that since the required actuator force is now 10% of the unassisted value, we can exploit the form of Fig. 12, and realise that we can substantially increase the stroke performed by just a single

	$\hat{a} = 0.5$	$\hat{a} = 0.8$
N	2	2
d mm	0.97	1.4
D mm	5.7	6.0
k kN /m (achieved)	23.0	85.5
Mass per spring g	1.94	4.48

Table 4   Optimised spring geometry.

actuator, and remove the need to have two actuators in series. In either approach the system mass is highly likely to be reduced. Even though the mass of the PEB mechanism is likely to be several times higher than that of the springs alone, due to the specific energy comparison between actuator and PEB, it seems highly probable that an overall mass saving at the system level will be achieved.

V. Conclusions

This work has highlighted how the Passive Energy Balancing concept can be applied and optimised for both dynamic and quasistatic actuation. It has considered the PEB device as a form of local energy storage, and used the overall amount of stored potential energy as a proxy for the mass of the PEB, to be used in optimisation. This method of optimisation is useful because it considers the mass penalty of the PEB device itself; not just its benefits in reducing actuator duty. Furthermore, it highlights that an optimal PEB device will often be strongly nonlinear, and that the ultimate mass of the PEB will be highly dependant on the specific strain energy of the material used, and structural form, of the elements used for energy storage.

The work then considered system level evaluation and optimisation, and considered that PEB could potentially reduce system mass both through fuel saving and reductions to actuator mass. The first saving would only give overall mass benefits after a certain number of actuator cycles had been performed on a given mission. Actuator mass saving may be impossible in the case of some actuators with high specific work capacities, but for many other actuators is easy to achieve if the actuator's specific work capacity is significantly lower than the maximum specific strain energy of the material used for energy storage.

A case study showed, that in the case of an amplified piezoelectric actuator, a simple PEB mechanism could significantly reduce maximum force and work requirement, and save significant actuator mass. The particular form of the stroke/force profile for these actuators meant that PEB was particularly useful in enabling the actuator to use more of its available stroke, because the maximum required actuator force was so much lower.

A. Finding the stroke that gives maximum force reduction for the snap through PEB

To find the maximum force, it is necessary to find the turning point of Eq. (22). First the Eq. is nondimensionalised using

$$\hat{x} = \frac{x}{\ell_0} \tag{26}$$

and

$$\hat{P}_n(\hat{x}) = \frac{P_n(\ell_0 \hat{x})}{k\ell_0} = 2\hat{x}\left(1 - \frac{1}{\sqrt{\hat{a}^2 + \hat{x}^2}}\right) , \tag{27}$$

where $\hat{a} = a/\ell_0$. Differentiating and equating to zero at $\hat{x} = \hat{x}_0$ gives

$$\frac{\mathrm{d}\hat{P}_n}{\mathrm{d}\hat{x}}\bigg|_{\hat{x}=\hat{x}_0} = 2\left(1 - \left(\frac{1}{\sqrt{\hat{a}^2 + \hat{x}_0^2}} - \frac{\hat{x}^2}{\left(\hat{a}^2 + \hat{x}_0^2\right)^{3/2}}\right)\right) = 0 . \tag{28}$$

This rearranges to

$$\sqrt{\hat{a}^2 + \hat{x}_0^2}\left(\hat{a}^2 + \hat{x}_0^2\right) = \hat{a}^2 . \tag{29}$$

Squaring both sides and collecting terms gives

$$\hat{x}_0^6 + 3\hat{a}^2\hat{x}_0^4 + 3\hat{a}^4\hat{x}_0^2 + \hat{a}^6 - \hat{a}^4 = 0 \ . \tag{30}$$

Acknowledgments

References

[1] Barbarino, S., Bilgen, O., Ajaj, R. M., Friswell, M. I., and Inman, D. J., "A review of morphing aircraft," *Journal of Intelligent Material Systems and Structures*, Vol. 22, No. 9, 2011, pp. 823–877.

[2] Majeti, R. K., van der Wall, G., B., and Balzarek, C. G., "Linearly variable chord-extension morphing for helicopter rotor blades," *CEAS Aeronaut Journal*, Vol. 12, 2021, pp. 55–67.

[3] Straub, F. K., "A feasibility study of using smart materials for rotor control," *Smart Materials and Structures*, Vol. 5, No. 1, 1996, p. 1.

[4] Grohmann, B., Maucher, C., and Jänker, P., "Actuation concepts for morphing helicopter rotor blades," *25th International Congress of the Aeronautical sciences*, 2006, pp. 3–8.

[5] Stewart, W., "Second harmonic control on the helicopter rotor," Tech. rep., Aeronautical Research Council, 1952.

[6] Woods, B. K., and Friswell, M. I., "The Adaptive Aspect Ratio morphing wing: Design concept and low fidelity skin optimization," *Aerospace Science and Technology*, Vol. 42, 2015, pp. 209 – 217.

[7] Woods, B. K. S., and Friswell, M. I., "Spiral pulley negative stiffness mechanism for passive energy balancing," *Journal of Intelligent Material Systems and Structures*, Vol. 27, No. 12, 2016, pp. 1673–1686.

[8] Zhang, J., Shaw, A. D., Amoozgar, M., Friswell, M. I., and Woods, B. K. S., "Bidirectional torsional negative stiffness mechanism for energy balancing systems," *Mechanism and Machine Theory*, Vol. 131, 2019, pp. 261–277.

[9] Zhang, J., Shaw, A. D., Amoozgar, M., Friswell, M. I., and Woods, B. K. S., "Spiral Pulley Negative Stiffness Mechanism for Morphing Aircraft Actuation," *ASME 2018 International Design Engineering Technical Conferences and Computers and Information in Engineering Conference*, American Society of Mechanical Engineers, 2018, pp. V05BT07A003–V05BT07A003.

[10] Zhang, J., Shaw, A. D., Amoozgar, M., Friswell, M. I., and Woods, B. K. S., "Bidirectional Spiral Pulley Negative Stiffness Mechanism for Passive Energy Balancing," *Journal of Mechanisms and Robotics*, Vol. 11, No. 5, 2019.

[11] Zhang, J., Wang, C., Shaw, A. D., Amoozgar, M., and Friswell, M. I., "Passive energy balancing design for a linear actuated morphing wingtip structure," *Aerospace Science and Technology*, Vol. 107, 2020, p. 106279.

[12] Huber, J., Fleck, N., and Ashby, M., "The selection of mechanical actuators based on performance indices," *Proceedings of the Royal Society of London A: Mathematical, Physical and Engineering Sciences*, Vol. 453, No. 1965, 1997, pp. 2185–2205.

[13] Zupan, M., Ashby, M. F., and Fleck, N. A., "Actuator classification and selection—the development of a database," *Advanced Engineering Materials*, Vol. 4, No. 12, 2002, pp. 933–940.

[14] Cebon, D., and Ashby, M. F., "The optimal selection of engineering entities," Tech. rep., Cambridge Engineering Design Centre, 1997.

[15] Zahoor, Y., De Breuker, R., and Voskuijl, M., "Preliminary Design of a Trailing Edge Morphing Surface for Rotorcraft," *AIAA SciTech Forum*, Orlando, FL, 2020.

[16] Mkhoyan, T., Thakrar, N. R., De Breuker, R., and Sodja, J., "Design and Development of a Seamless Smart Morphing Wing Using Distributed Trailing Edge Camber Morphing for Active Control," *AIAA Scitech 2021 Forum*, 2021, p. 0477.

[17] ANSYS, Inc, "Granta Edupack 2020 Version 20.1.0," , 2021.

[18] Nojoumi, H., Dincer, I., and Naterer, G. F., "Greenhouse gas emissions assessment of hydrogen and kerosene-fueled aircraft propulsion," *International Journal of Hydrogen Energy*, Vol. 34, No. 3, 2009, pp. 1363–1369.

[19] Ansys Granta, "Teaching resources," , 2021. `https://www.grantadesign.com/teachingresource/type/` accessed November 2021.

[20] Werter, N., Sodja, J., Spirlet, G., and De Breuker, R., "Design and experiments of a warp induced camber and twist morphing leading and trailing edge device," *24th AIAA/AHS adaptive structures conference*, 2016, p. 0315.

[21] Cedrat Technologies, "Amplified piezo actuator," , 2021. `https://www.cedrat-technologies.com/en/products/product/APA1500L.html`, accessed November 2021.